Available online at www.sciencedirect.com

ScienceDirect

Polymer 49 (2008) 1611–1619

polymer

www.elsevier.com/locate/polymer

Preparation of skinless polymer foam with supercritical carbon dioxide and its application to a photoinduced hydrogen evolution system

M. Morisaki [a], T. Ito [a], M. Hayvali [b], I. Tabata [c], K. Hisada [a,*], T. Hori [a]

[a] *Fiber Amenity Engineering Course, Graduate School of Engineering, University of Fukui, 3-9-1 Bunkyo, Fukui-shi, Fukui 910-8507, Japan*
[b] *Department of Chemistry, Ankara University, 06100 Tandogan-Ankara, Turkey*
[c] *Department of Technology, Faculty of Engineering, University of Fukui, 3-9-1 Bunkyo, Fukui 910-8507, Japan*

Received 25 July 2007; received in revised form 4 January 2008; accepted 19 January 2008
Available online 29 January 2008

Abstract

Skinless polymer foam was prepared by treating poly(methyl methacrylate) (PMMA) with supercritical carbon dioxide ($scCO_2$). The film was immersed in $scCO_2$ with ethanol to nucleate, and then incubated in a hot water bath to induce nuclear growth and to prepare skinless PMMA foam. The obtained polymer foam had a low density and cells were connected to each other to make channels through the skin layer. Low molecular weight PMMA formed skinless foam with larger cells through expansion. PMMA film containing tin *meso*-tetraphenyl porphyrin was also foamed with same procedure and the foam was used for photoinduced hydrogen evolution. A larger amount of hydrogen evolved from the photocatalyst on the skinless PMMA foam in comparison with the foam with skin. Enlargement of effective surface area of solid support and light scattering within the foam could enhance turnover number (TON) of photocatalyst.

Keywords: Supercritical fluid; Skinless foam; Hydrogen evolution

1. Introduction

Photocatalytic water splitting is a challenging reaction to supply hydrogen from a sustainable source. Tetraphenyl porphyrin (TPP), phthalocyanine and bipyridyl complex were studied as organic dyes for photoinduced hydrogen evolution. Wang et al. reported that tin tetraphenyl porphyrin (SnTPP) acts as an effective photocatalyst for photoinduced hydrogen evolution with visible light [1]. Compared to other organic dyes, SnTPP has some advantages in the photoinduced hydrogen evolution system with polymer solid. TPP dissolves in various organic solvents compared with phthalocyanine, and it can readily disperse in polymer matrix. The molar extinction coefficient of TPP has larger value than that of tris(2,2′-bipyridyl) ruthenium complex in a visible light region.

While SnTPP is stable against light irradiation among metalloporphyrins, irradiation of intense light onto its solution causes degradation of SnTPP. The durability of the dye can be extended by immobilizing the dye on a solid support [2–4]. Immobilization of SnTPP on the solid might reduce the chance of photocatalyst to contact with other reactants such as water and electron donors which may inhibit the hydrogen evolution photoreaction. Some studies paid attention to the morphology of the solid support in order to increase the efficiency of photoreaction on the solid support. Porous material is attractive as a catalyst because of the ability to absorb and interact with atoms, ions and molecules such as zeolite/silica [5] and polymer/silica [6]. Rachel and coworkers used pumice stone as a solid support [7].

Supercritical carbon dioxide ($scCO_2$) fluid is a tunable medium that can be used as an additive in polymer processing [8–10]. For example, $scCO_2$ has been used as a foaming agent for polymers such as polystyrene [11], polycarbonate [12], poly(ethylene terephthalate) [13], poly(ethylene-*co*-vinyl acetate) [14] and PMMA [15,16]. Average cell size and bulk

---

* Corresponding author. Tel.: +81 776 27 8574; fax: +81 776 27 8747.
E-mail address: hisada@acbio2.acbio.fukui-u.ac.jp (K. Hisada).

0032-3861/$ - see front matter © 2008 Elsevier Ltd. All rights reserved.
doi:10.1016/j.polymer.2008.01.049

density can be varied by processing conditions, such as pressure, temperature and decompressing rate [17–19]. When the polymer matrixes were foamed with pure carbon dioxide, the resulting polymer foam had an unfoamed skin layer around the film surface [20]. Rapid diffusion out creates a skin layer near the edges in which the gas concentration is too low to contribute to nucleation of gas cells [15,21]. The skin layer blocks the penetration of reactant into the polymer foam, which reduces the apparent reactivity of the photocatalyst on the polymer matrix.

In this work, we prepared skinless PMMA foam with supercritical fluid. $scCO_2$ was used as an inert foaming agent because it did not inhibit the photoreaction. Our strategy to prepare skinless foam was: (1) to add a modifier into $scCO_2$, (2) to treat the $scCO_2$-impregnated film in hot water (foaming), and (3) to adjust the molecular weight of the matrix polymer. The foamed films were applied as a solid support for inducing hydrogen evolution with visible light.

2. Experimental

2.1. Materials

Low molecular weight PMMA (LPMMA) and high molecular weight PMMA (HPMMA) were provided by Wako Pure Chemical Industries Ltd. and Nacalai Tesque, Inc., respectively. They were used without further purification. The molecular weights of PMMAs were measured by GPC with polystyrene standards. Weight-average molecular weights were 1.72×10^5 and 1.12×10^6 for LPMMA and HPMMA, respectively. Carbon dioxide was obtained from Uno Sanso Co., Ltd. (>99.5% pure). TPP was obtained from Kanto Chemical Co. Ltd. 2-Mercaptoethanol and hexachloroplatinic acid (H_2PtCl_6) were purchased from Nacalai Tesque, Inc. All other reagents were of reagent grade and were used without further purification. SnTPP was synthesized by refluxing the mixture of tin(II) chloride dihydrate and TPP in *N*,*N*-dimethyl formamide [22]. The synthesized compounds were identified by ^{1}H NMR and UV–vis spectroscopies.

2.2. Foaming of photocatalytic film with supercritical carbon dioxide

A 10 wt% PMMA solution in toluene was casted onto a glass plate to obtain a film having ca. 100 μm in thickness. The cast film was dried for 24 h at ambient temperature, and then placed in a vacuum oven at 50 °C for 24 h and at room temperature for 24 h. The dried film was cut into 12 cm^2 pieces (3 cm × 4 cm) for foaming experiments. SnTPP was doped into PMMA film by casting PMMA onto the glass plate with SnTPP. An organic dye, SnTPP, was compatible to PMMA and was dispersed in the PMMA matrix without aggregation of SnTPP.

A supercritical carbon dioxide extraction system (ISCO-2200) was applied for impregnation of carbon dioxide at a supercritical condition. Fig. 1 shows the schematic illustration of the apparatus. The cast films were set in a high-pressure column (10.89 mL) and the entire column was placed in a thermostat oven. The temperature in the oven was held constant from 30 to 80 °C. At a given temperature, CO_2 was fed into the column from a high-pressure pump until a target pressure, 15–25 MPa, is reached. A small amount of ethanol was added to $scCO_2$ as a co-solvent; 0–7.5 mol% of CO_2.

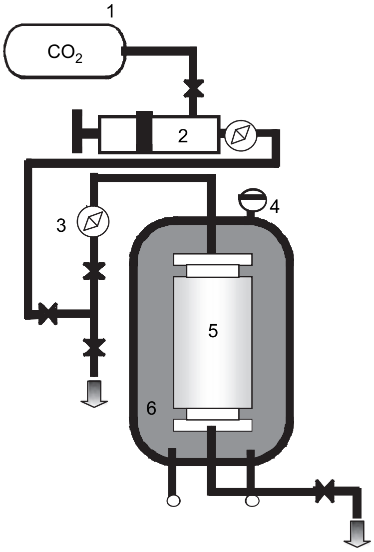

Fig. 1. Schematic representation of foaming equipment with (1) carbon dioxide feed, (2) cylindrical pump, (3) pressure gauge, (4) temperature indicator, (5) high-pressure column, and (6) thermostat bath.

The supercritical fluid was impregnated into PMMA film at the target pressure, for 5 to 60 min. After $scCO_2$ impregnation, the vessel was depressurized at a rate of 1.3 MPa s^{-1} and the film was immediately dipped into water at 95 °C for 2 min. During the heating process, CO_2 bubble expanded in the PMMA films. The foamed film was quenched in cool water at 20 °C to fix the porous structure. The PMMA films were dried under vacuum at 50 °C for 2 h.

2.3. Characterization of the PMMA foam

The morphology of PMMA foam was observed with a scanning electron microscope (SEM, Hitachi-2600 electron microscope). SEM images gave us information about cell structure and thickness of skin layer (the unfoamed layer surrounding the foam). Pt/Pd was sputtered on the film to avoid the charge up of specimen. Images were acquired at an acceleration voltage of 15 kV. The density of the polymer foam was measured with an electronic densitometer EW-300SG (Alfa Mirage Co. Ltd.).

2.4. Photochemical assay

PMMA film and PMMA foams were dried under vacuum at 50 °C for 2 h, and then they were used in a photoinduced hydrogen evolution system. The sample mixture of photoinduced hydrogen evolution was composed of 2-mercaptoethanol (an electron donor), Pt colloid and PMMA foam containing 1-μmol SnTPP as a photosensitizer. The hexachloroplatinic acid (H_2PtCl_6) was reduced to metal Pt with sodium citrate [23]. The reaction mixture was put in an optical cell and the headspace in the optical cell was kept to 700 μL. Nitrogen gas was bubbled into the aqueous solution to remove oxygen in the system just before the irradiation. The optical cell in a thermostat water bath (30 °C) was irradiated with a 300-W tungsten lamp (Philips-JCR). A Toshiba L-39 filter was used to ensure that only visible light ($\lambda > 390$ nm) was irradiated on the sample. The quantum input rate into the optical cell was measured as 0.23 mmol L^{-1} s^{-1} with a standard oxalate actinometry. The generated gas was collected with a gastight syringe, and the amount of hydrogen evolution was analyzed by gas chromatograph (Hitachi G-3000), which was composed of molecular sieve 5 Å (60/80) column and thermal conductivity detector [5].

3. Results and discussion

3.1. Preparation of skinless polymer foam

Supercritical fluid was impregnated into a polymer film and then the impregnated carbon dioxide was expanded at ambient pressure. The film was foamed as follows: (1) polymer film was saturated with supercritical carbon dioxide fluid at a high pressure (15–25 MPa); (2) polymer/gas mixture was quenched into a supersaturated state by reducing the pressure (pressure quench), phase separation took place between the polymer-rich and gas-rich phases to form cell nuclei; and (3) nuclear growth of gas cells within the polymer film. When PMMA film was foamed with pure carbon dioxide, trace amounts of gas cells formed around the middle of the film as shown in Fig. 2 (Foam I). We improved the foaming step to make foam without a skin layer which disturbs the penetration of reactant, and a larger cell is preferred for the smooth penetration of aqueous solution. The foam's morphology will be affected by increasing CO_2 sorption because large sorption of CO_2 causes density fluctuation of CO_2 to be larger in PMMA film, which will produce PMMA foam containing cells percolating from the surface to the middle of the foam. Hirogaki et al. reported that addition of polar modifiers, *i.e.*, alcohol or acetone, increased the affinity of the CO_2 fluid for PET [24]. The following three factors were investigated to enlarge the cells in polymer foam and to prepare an efficient solid support for hydrogen evolution: (1) addition of modifier with $scCO_2$, (2) additional treatment in hot water (foaming), and (3) molecular weight of matrix polymer.

Fig. 2 shows a sectional view of HPMMA casted film and foam prepared by four procedures. Each foam was treated with $scCO_2$ at 50 °C and 20 MPa for 15 min. Foam II was obtained by exposing HPMMA to $scCO_2$ containing adding 5 mol% of ethanol. Foam III was prepared by soaking Foam I in water at 95 °C just after $scCO_2$ sorption (foaming step). Similarly, Foam IV was prepared by soaking Foam II in a hot water bath.

3.1.1. Modification of $scCO_2$ with ethanol

As shown in Fig. 2, cells in Foam II were obviously larger than those in Foam I. Figs. 3 and 4 show the average cell diameter and the thickness of skin layer for PMMA foam prepared with $scCO_2$ containing from 1 to 7.5 mol% of ethanol as a co-solvent. PMMA film, treated with the modified CO_2, became foam with a larger cell diameter and the cell size showed a bimodal distribution (Fig. 3). Another feature of Foam II is that the thickness of skin layer decreased monotonously from 45 to 35 μm by adding ethanol in $scCO_2$ (Fig. 4).

The addition of ethanol into $scCO_2$ enhanced the affinity between cellulose derivatives and CO_2 fluid [25]. The result suggests that the addition of ethanol into $scCO_2$ could also enhance the affinity between semipolar PMMA and $scCO_2$. The skin layer on the polymer foam was formed through rapid release of CO_2 near the surface of polymer film. The decrease in the skin thickness is attributed to the delayed release of sorbed CO_2 from PMMA film. By increasing the affinity between $scCO_2$ and matrix polymer, the fluid was held in the PMMA film for a longer period. However, Foam II still had skin layer, and another procedure was required to prepare skinless PMMA foam.

3.1.2. Additional foaming in a hot water

Foam III was prepared from Foam I by additional foaming in hot water. The process made cells larger (13 ± 2.5 μm) and made the density of the foam lower than those for Foam I (Table 1). The thickness of the skin layer decreased to 10 ± 1.0 μm, but the top surface of the Foam II was covered by dense skin layer.

3.1.3. Modification of $scCO_2$ with ethanol and additional foaming in a hot water

The additional foaming for Foam II lowered the density of the foam as shown in Table 1. Cells in Foam IV-i have larger cell diameters and some of them were coalesced to make huge cell by both ethanol addition into $scCO_2$ and nuclear growth in hot water (Fig. 2). Fig. 5 shows PMMA foam prepared with $scCO_2$ containing 0.1–5.0 mol% of ethanol as a co-solvent. The cell size showed unimodal distribution when PMMA film was treated with pure $scCO_2$ (Fig. 3(a)). When PMMA films treated with $scCO_2$ containing more than 0.1 mol% of ethanol, cell sizes showed a bimodal distribution. Both diameters of larger cells and the fraction of them increased in the foam with the concentration of ethanol in $scCO_2$. After pressure quench, the sorbed film was phase separated to CO_2-rich phase and polymer-rich phase. The increase in CO_2 sorption could make larger density fluctuation of CO_2 in PMMA film. When CO_2 sorption was not sufficient, only CO_2-rich phase contained CO_2 enough to nucleate. On the other hand, the polymer-rich phase could also nucleate when supercritical fluid sorbed in polymer film by adding ethanol. At this stage, larger cells come from the CO_2-rich phase and smaller cells from the polymer-rich phase. Therefore, addition of ethanol in $scCO_2$ resulted in bimodal distribution of cell diameters.

Fig. 6 shows PMMA films foamed in a hot water at 95 °C for 1–120 s after they were impregnated with $scCO_2$ containing 5.0 mol% of ethanol. As the foaming time was prolonged, the cell diameter became larger and was saturated around

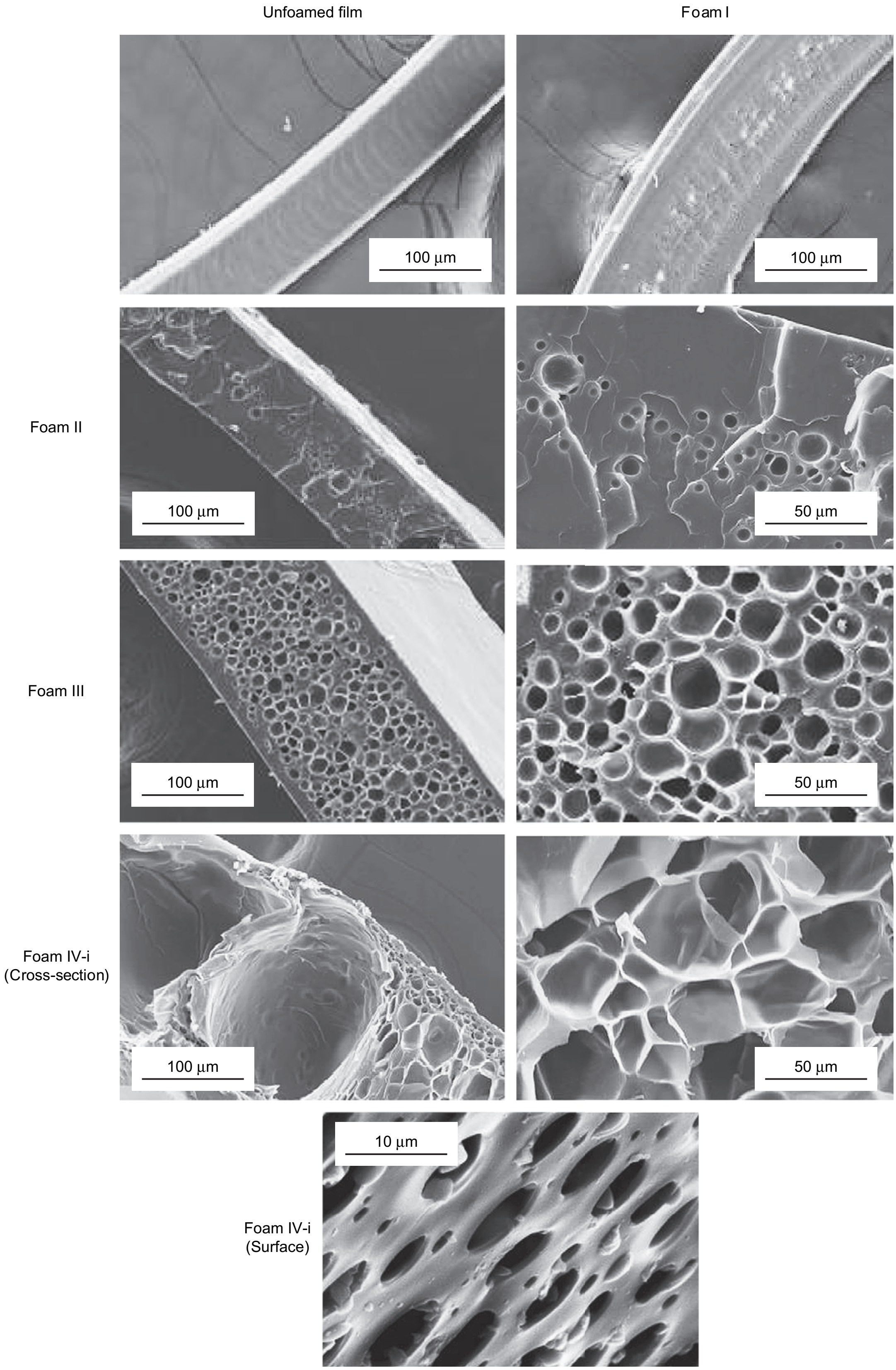

Fig. 2. SEM images of PMMA cast film and PMMA foam. PMMA foam prepared with $scCO_2$ at 50 °C and 20 MPa for 15 min. The image on the right side shows an enlarger view of the image on the left side. Bottom image is the surface view of Foam IV-i.

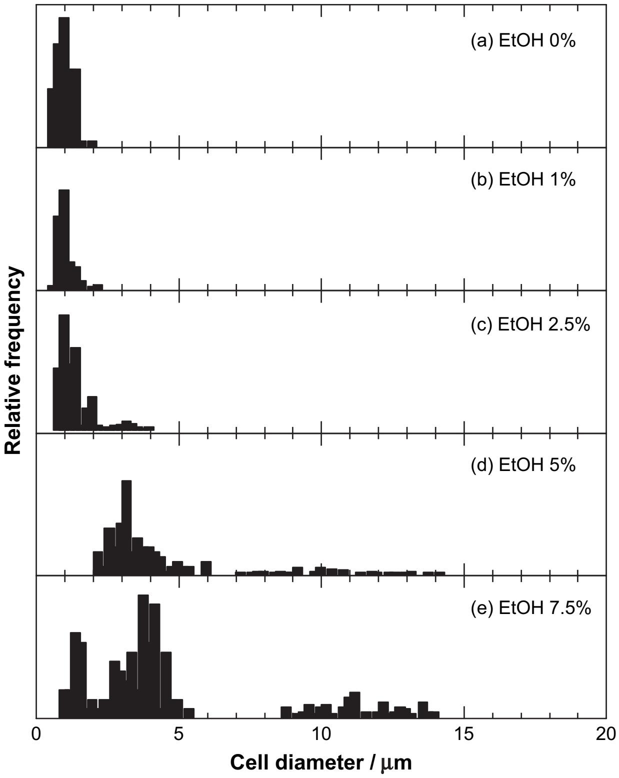

Fig. 3. Cell size distribution in PMMA foam prepared with $scCO_2$ at 20 MPa and 50 °C for 15 min. The additive in the supercritical fluid was (a) none, (b) 1.0% ethanol, (c) 2.5% ethanol, (d) 5.0% ethanol and (3) 7.5% ethanol.

Table 1
Density and thickness of skin layer for PMMA foams prepared with $scCO_2$

Foam	Density/g cm^{-3}	Thickness of skin layer/μm
Cast film[a]	1.18	–
Foam I[a]	1.01	47.2 (±2.3)
Foam II[a]	0.97	37.4 (±2.4)
Foam III[a]	0.66	10.1 (±1.0)
Foam IV-i[a]	0.49	0
Foam IV-ii[b]	0.06	0

[a] Prepared with HPMMA ($M_w = 1.12 \times 10^6$).
[b] Prepared with LPMMA ($M_w = 1.72 \times 10^5$).

120 s. The viscosity of the polymer matrix decreased at elevated temperature, and nuclear bubbles coalesced each other to enlarge cell diameters in the foaming process. As shown in Fig. 2, the side view of Foam IV-i shows that the cells formed channels through the entire foam and the channel reached the surface of polymer foam. The foam had no skin layer anymore and percolation of channel enhanced the reactive surface area, which can improve the ability of polymer foam as photoreactor.

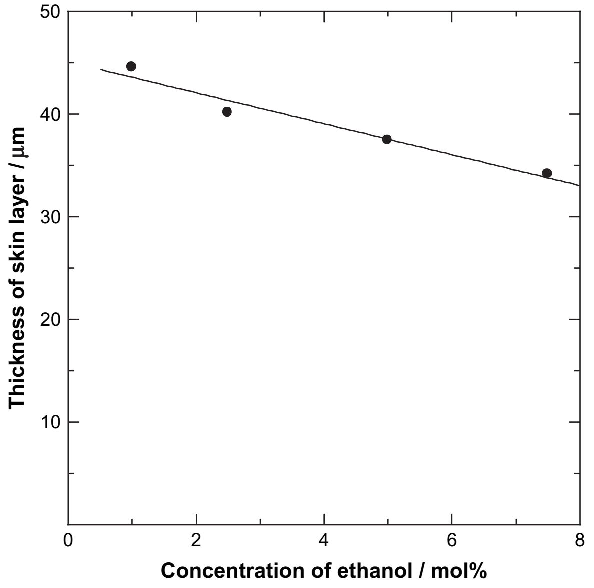

Fig. 4. Effect of ethanol addition into $scCO_2$ on the thickness of skin layer. The PMMA foam was prepared with $scCO_2$ at 20 MPa and 50 °C for 15 min.

3.1.4. Effect of molecular weight of polymer on foaming

Fig. 7 shows polymer foams prepared from PMMAs having different molecular weights. The weight-average molecular weights of HPMMA and LPMMA were 1.12×10^6 and 1.72×10^5, respectively. Though skinless foam could be prepared from both polymers, the density of LPMMA foam (0.06 g cm^{-3}) was less than the one for HPMMA foam (0.49 g cm^{-3}). The number density of cells decreased and the wall between the cells became thinner in the LPMMA foam (Foam IV-ii). Colton and Suh discussed that lower molecular weight polymers had fewer nucleation sites using the classical nucleation theory [26–28]. Taki et al. measured the steady shear viscosity of polypropylene (PP) having different molecular weight in $scCO_2$. The shear viscosity for low molecular weight PP ($M_w = 1.84 \times 10^5$) was more than one order of magnitude lower than those for high molecular weight PP ($M_w = 6.10 \times 10^5$) [29]. In this system, carbon dioxide diffused out from the matrix after pressure quench, and the viscosity of the matrix gradually increased with an elapse of time. At the same CO_2 sorption, the viscosity of LPMMA matrix is around one-sixtieth of that for HPMMA matrix [30,31]. The low viscosity will lead to larger expansion and coalesce of cells during the foaming process. Therefore, LPMMA foam has larger specific surface area and more photocatalysts exist on the surface of cell when SnTPP-doped PMMA was foamed by this foaming procedure.

3.2. Photoinduced hydrogen evolution with the foamed film system

PMMA foams were prepared from SnTPP-doped PMMA film, and the foam was applied to the photoinduced hydrogen evolution system. Fig. 8 shows the hydrogen evolution from SnTPP on PMMA foam with the elapse of time. When the unfoamed film was used as solid support, 2.3 μL of hydrogen evolved after a 30-h irradiation. When Foam I and Foam II were used as solid support, the system evolved 0.9 and 2.5 μL of hydrogen, respectively. These two foams did not increase the efficiency of photoreaction at the interface of polymer and aqueous media. When Foam III was used in the hydrogen evolution system, it evolved 3.5 μL of hydrogen

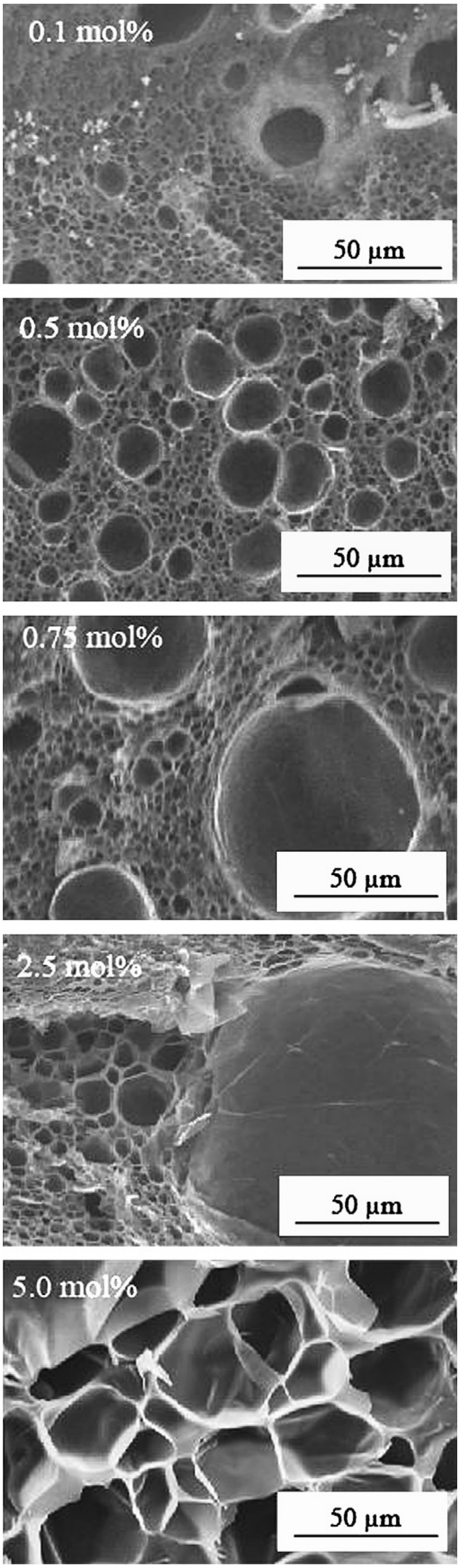

Fig. 5. Effect of ethanol addition into $scCO_2$ on cell structure in PMMA foams. The foam heated at 95 °C after the impregnation of $scCO_2$ with ethanol at 50 °C and 20 MPa for 15 min.

after a 30-h irradiation. Beside surface area enlargement, microcellular foam scatters incident light in the foam [32]. The diffuse reflection of the irradiated light increases the frequency of collision between photon and photocatalyst, which is a factor to enlarge the reaction yield on Foam III. For Foam III, the amount of hydrogen evolution slightly increased in comparison with those for other PMMA foams with skin, Foam I or Foam II. When skinless Foam IV-i was used as photoreactor, SnTPP evolved 9.1 μL of hydrogen, which is about four times larger than that for the unfoamed film. Dense skin layer on the polymer foam blocked the diffusion of reactant onto the reaction site in the foam even if the polymer foam had enough cells in their interior. Skinless foam, Foam IV, enabled the reactant to penetrate onto the reaction site.

Table 2 summarizes the maximum amounts of hydrogen evolution and induction times of photoreaction for SnTPP-doped PMMA foam. The maximum hydrogen evolution was estimated from the first-order reaction kinetics. On Foam IV-i, SnTPP reacted with a shorter induction time and larger maximum hydrogen evolution. In the induction period, the aqueous solution penetrated through the microchannel and the system reached an equilibrium state for the inhomogeneous reaction between reactant in the aqueous phase and photosensitizer SnTPP on the polymer solid. The foam morphology might accelerate the diffusion of reactant to the reaction site in Foam IV-i.

Fig. 9 shows the hydrogen evolution from Foam IV prepared with LPMMA (Foam IV-ii) and HPMMA (Foam IV-i). After a 30-h irradiation, HPMMA and LPMMA foams evolved 9.1 and 16.9 μL of hydrogen, respectively. When Foam IV-i was applied in the photoinduced hydrogen evolution system, induction time was 2.8 h before hydrogen evolution. On the other hand, photocatalyst on Foam IV-ii evolved hydrogen immediately after photo-irradiation. Penetration of a liquid into a capillary is expressed with the Lucas–Washburn equation:

$$x^2 = \frac{r\gamma_{LV}\cos\theta}{2\eta}t \qquad (1)$$

where x denotes the distance penetrated by the liquid, γ_{LV} the surface tension of the liquid of viscosity η, θ the contact angle between the liquid and the capillary surface, r the internal radius of the capillary, and t the penetration time [33,34]. For Foam IV-i and Foam IV-ii, the penetrated distance of water was estimated by average pore radii. The penetrated distance for Foam IV-ii was ca. 25% longer than that for Foam IV-i during the same reaction period. In the present reaction system, reactants diffuse onto the reaction site within the polymer foam through the flow of aqueous solution. Then, the reactants could reach the reaction site more rapidly for Foam IV-ii. As shown in Fig. 7, Foam IV-ii had a thinner cell wall, which means that it had a larger surface than Foam IV-i. The lower density of Foam IV-ii also supports that this interpretation would be valid for whole of Foam IV-ii not only in a view area of microscopy. While

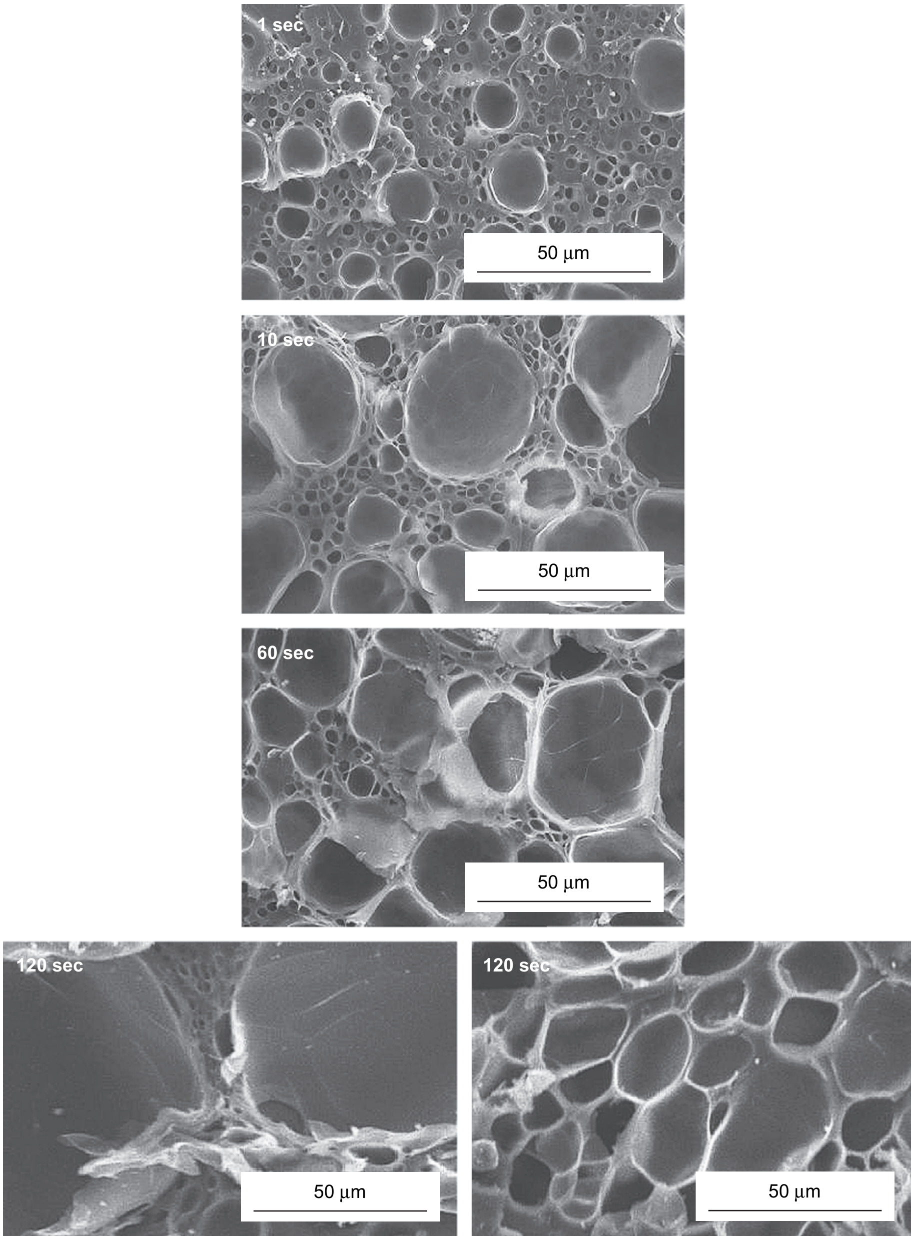

Fig. 6. Effect of foaming time on morphology of PMMA foam. The foam heated at 95 °C after the impregnation of $scCO_2$ with 5 mol% of ethanol at 50 °C and 20 MPa for 15 min.

Foam IV-i and Foam IV-ii contained the same amount of photocatalysts, a larger fraction of photocatalyst existed on the surface of Foam IV-ii, because Foam IV-ii has a larger surface/bulk ratio. The photocatalyst in the bulk cannot react with the reactant in the aqueous solution, so the larger surface/bulk ratio increased the reaction rate of photoinduced hydrogen evolution. Fast penetration of aqueous phase and large specific surface area caused more than 1.8 times evolution of hydrogen from SnTPP on the Foam IV-ii system than that on the Foam IV-i system.

In this work, turnover number (TON) was defined as an index for efficiency of hydrogen evolution among various polymer supported system. The TON of hydrogen evolution can be defined by the following equation:

$$\begin{aligned}\mathrm{TON} &= \frac{\text{The number of reacted photoelectrons}}{\text{The amount of tin porphyrin}}\\ &= \frac{\text{The mole of evoluted } \mathrm{H_2}\ (\mathrm{mol}) \times 2}{\text{The mole of tin porphyrin (mol)}}\end{aligned} \qquad (2)$$

TON was calculated under the assumption that all the porphyrin in the solid related to the photoreaction. The assumption is not exactly valid for the present system, but we can compare the reaction efficiency of organic photocatalyst on other polymer system by using TON. In this system, TONs were 1.3 and 2.4 for Foam IV-i and Foam IV-ii, respectively. TON of hydrogen evolution was reported for chlorophyll *a*-FSM [5], RuQPIm free-standing film containing MV^{2+} system [4] and chlorophyll *a*-PVP–SME [2] as 0.10, 2.1 and 1.9,

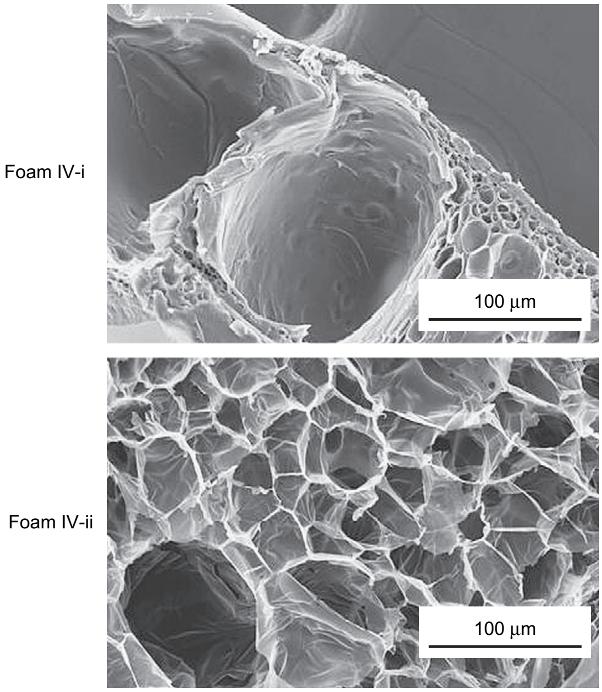

Fig. 7. SEM images of PMMA foam having different molecular weights. The foam heated at 95 °C after the impregnation of $scCO_2$ with 5 mol% of ethanol at 50 °C and 20 MPa for 15 min. Molecular weights of PMMA are 1.12×10^6 (Foam IV-i), or 1.72×10^5 (Foam IV-ii).

respectively. TON of SnTPP on this skinless foam systems was almost of the same order of magnitude even if semipolar PMMA was used as supporting solid.

4. Conclusion

In this study, SnTPP-doped skinless polymer foam was prepared with $scCO_2$ and examined for photoinduced hydrogen evolution. Various foamed structures were obtained by changing the preparation conditions: addition of ethanol in $scCO_2$ and foaming process in a hot water bath, and molecular weight of matrix polymer. The resulting polymer foam had a low density and cells were connected to each other to make channels through the skin layer. Low molecular weight LPMMA formed foam with larger cells through expansion. The number density of cells decreased and the wall between the cells became thinner in the LPMMA foam (Foam IV-ii). When the skinless PMMA foam was used as the solid support for photocatalyst, a larger amount of hydrogen evolved than that from SnTPP on the PMMA foam. Hydrogen evolution from the LPMMA foam was 1.8 times more rapid than that from the HPMMA foam. TON of SnTPP on this skinless foam system was 2.4 though the value was estimated including SnTPP in the PMMA bulk.

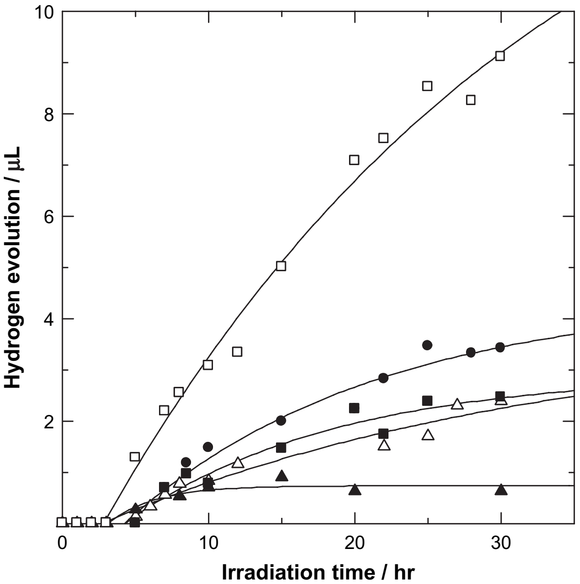

Fig. 8. Hydrogen evolution from SnTPP-doped PMMA foam: Foam I (▲), Foam II (■), Foam III (●), Foam IV-i (□) and cast film (△).

Table 2
Maximum hydrogen evolution and induction time for the photoinduced hydrogen evolution from the SnTPP-doped PMMA foam

Foam	Maximum hydrogen evolution/μL	Induction time/h
Cast film[a]	2.54	3.80
Foam I[a]	0.74	3.11
Foam II[a]	3.07	4.20
Foam III[a]	4.42	4.23
Foam IV-i[a]	15.8	2.82
Foam IV-ii[b]	29.2	0

[a] Prepared with HPMMA ($M_w = 1.12 \times 10^6$).
[b] Prepared with LPMMA ($M_w = 1.72 \times 10^5$).

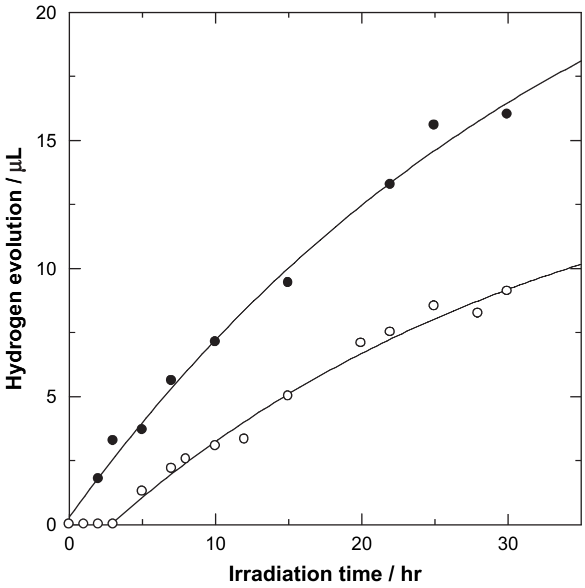

Fig. 9. Effect of molecular weight on photoinduced hydrogen evolution from SnTPP-doped PMMA foams. Molecular weights for PMMA were 1.72×10^5 (Foam IV-ii, ●) and 1.12×10^6 (Foam IV-i, ○).

References

[1] Wang S, Tabata I, Hisada K, Hori T. Dyes Pigments 2002;55:27–33.
[2] Itoh T, Ishii A, Kodera Y, Matsushima A, Hiroto M, Nishimra H, et al. Bioconjugate Chem 1998;9:409–12.

[3] Wang S, Tabata I, Hisada K, Hori T. J Porphyrins Phthalocyanines 2003;7:199–204.
[4] Suzuki M, Kobayashi S, Uchida S, Kimura M, Hanabusa K, Shirai H. Polymer 1998;39:1539–43.
[5] Itoh T, Yano K, Inada Y, Fukushima Y. J Am Chem Soc 2002;124: 13437–41.
[6] Wakayama H, Inagaki S, Fukusima Y. J Am Ceram Soc 2002;85:161–4.
[7] Rachel A, Lavedrine B, Subrahmanyam M, Boule P. Catal Commun 2002;3:165–71.
[8] Cooper AI. J Mater Chem 2000;10:207–34.
[9] West BL, Kazarian SG, Vincent MF, Brantly NH, Eckert CA. J Appl Polym Sci 1997;69:911–9.
[10] Wang Y, Yang C, Tomasko DL. Ind Eng Chem Res 2001;41:1780–6.
[11] Siripurapu S, Gay YJ, Royer JR, Desimone JM, Spontak RJ, Khan SA. Polymer 2002;43:5511–20.
[12] Beckman EJ, Goel SK. Cell Polym 1993;12:251–4.
[13] Baldwin DF, Shimbo M, Suh NP. J Eng Mater Technol 1995;117:62–4.
[14] Jacobs MA, Kemmere MF, Keurentjes JTF. Polymer 2004;45:7539–47.
[15] Goel SK, Beckman EJ. Polym Mater Sci Eng 1992;67:506–7.
[16] Siripurapu S, Desimone JM, Khan SA, Spontak RJ. Adv Mater 2004;16:989–94.
[17] Kumar V. Polym Eng Sci 1990;30:1323–9.
[18] Matsuyama H, Yano H, Maki T, Teramoto M, Mishima K, Matsuyama K. J Membr Sci 2002;194:157–63.
[19] Reverchon E. Polym Eng Sci 2006;4:188–98.
[20] Srinivas S, John AC, Richard JS, Saad AK. Macromolecules 2004;37: 9872–9.
[21] Goel SK, Beckman EJ. Polym Eng Sci 1994;34:1137–47.
[22] Whitten DG, Yau JC, Carroll FA. J Am Chem Soc 1971;93:2291–6.
[23] Amao Y, Kamachi T, Okura I. J Porphyrins Phthalocyanines 1998;2: 201–7.
[24] Hirogaki K, Tabata I, Hisada K, Hori T. J Supercrit Fluids 2005;36: 166–72.
[25] Kian K, Pohler H. J Supercrit Fluids 1998;13:135–47.
[26] Colton JS, Suh NP. Polym Eng Sci 1987;27:485–92.
[27] Colton JS, Suh NP. Polym Eng Sci 1987;27:493–9.
[28] Colton JS, Suh NP. Polym Eng Sci 1987;27:500–9.
[29] Taki K, Tabata K, Kihara S, Ohshima M. Polym Eng Sci 2006;46: 680–90.
[30] Fox Jr TG, Flory PJ. J Am Chem Soc 1948;70:2384–91.
[31] Fox Jr TG, Flory PJ. J Phys Colloid Chem 1951;55:221–8.
[32] Kabumoto A, Yoshida N, Itoh M, Okada M. US Patent 5,844,731; 1998.
[33] Washburn EW. Phys Rev 1921;17:273–83.
[34] Lucas R. Kolloid Z 1918;23:15–22.